Available online at www.sciencedirect.com
SCIENCE DIRECT®
Journal of Organometallic Chemistry 682 (2003) 73–78
Journal of Organometallic Chemistry
www.elsevier.com/locate/jorganchem

Heterometallic multinuclear Pt–M (M = Au, Ag) structural assemblies from dinuclear $[Pt_2(P–P)_2(\mu\text{-}S)_2]$ (P–P = 2PPh$_3$, dppf)

Zhaohui Li [1], K.F. Mok, T.S. Andy Hor *

Department of Chemistry, National University of Singapore, 3 Science Drive 3, Kent Ridge, Singapore 117543, Singapore

Received 1 June 2003; received in revised form 7 July 2003; accepted 15 July 2003

Abstract

Three heterometallic Pt–M (M = Ag, Au) complexes, viz. $[Au_2\{Pt_2(PPh_3)_4(\mu_3\text{-}S)_2\}_2]Cl_2$ (**2**), $Au_2Pt_2Cl_2(PPh_3)_4(\mu_3\text{-}S)_2$ (**3**) and $Ag_2Pt_2Cl_2(dppf)_2(\mu_3\text{-}S)_2$ (**4**) (dppf = 1,1′-bis(diphenylphosphino)ferrocene) were prepared from $Pt_2(P–P)_2(\mu\text{-}S)_2$(P–P = 2PPh$_3$ (**1a**), dppf (**1b**)) that has a butterfly $\{Pt_2S_2\}$ core. The structures of **2** and **4** were determined by X-ray single-crystal diffractometry. Complex **2** has a hexanuclear $\{Au_2Pt_4\}$ cage-framework comprising two hinged $\{Pt_2S_2\}$ anchored across strong Au–Au bond (2.837 Å). Complex **4** has a tetranuclear $\{Au_2Pt_2\}$ open-framework, which contains a flattened $\{Pt_2S_2\}$ butterfly with two AgCl 'molecular pendants' protruding perpendicularly out of the plane from the sulfur sites at opposite directions. The structural features of these polymetallic complexes and the synthetic and structural relationships between **2** and **3** are described.

Keywords: Heterometallic; Platinum, Gold; Silver; X-ray single-crystal crystallography; Sulfide; Structures

1. Introduction

The high nucleophilicity and stereoactive sulfur lone pairs in $Pt_2(PPh_3)_4(\mu\text{-}S)_2$ (**1a**) enabled us to develop a range of homo-, hetero- and inter-metallic sulfide complexes [1]. A notable example is the sequential growth of heteropolymetallic aggregates ($Pt_2 \rightarrow Pt_2Ag \rightarrow Pt_2Ag_2 \rightarrow Pt_4Ag_2$) that we demonstrated recently [2]. Apart from these structural assemblies, we are also interested in their functional behaviors such as electroactivities [3] and template function in organic syntheses [4]. In view of the structural diversity and chemical significance of d^8–d^{10} assemblies, we decided to extend our investigations to other Pt–Au/Ag assemblies in a hope to understand their structural distinctions and compare with other reported related systems [5].

2. Results and discussion

Complex **1a** reacts stoichiometrically with $AuCl(SMe_2)$ in 1:1 and 1:2 ratios to give $[Au_2\{Pt_2(PPh_3)_4(\mu_3\text{-}S)_2\}_2]Cl_2$, (**2**) and $Au_2Pt_2Cl_2(PPh_3)_4(\mu_3\text{-}S)_2$ (**3**), respectively. Complex **2** converts to **3** upon molar addition of $AuCl(SMe_2)$. This reaction can be reverted upon introduction of **1a**. The formation and interconversion pathways are summarized in Scheme 1.

The ligand lability in $AuCl(SMe_2)$ and the high aurophilicity of the sulfur centers in **1a** enables $AuCl(SMe_2)$ to function as a source for atomic gold. X-ray single-crystal diffraction analysis confirmed that **2** is a $\{Au_2Pt_4\}$ hexanuclear aggregate formed by two hinged-butterfly anchoring at opposite ends of two gold atoms (Fig. 1 and Table 1). The resultant $\{Au_2Pt_4S_4\}$ cage-framework illustrates its isostructural relationship to its related Ag(I) analogue $[Ag_2\{Pt_2(PPh_3)_4(\mu_3\text{-}S)_2\}_2]^{2+}$, which is however obtained from a 'ligand-free' substrate, viz. $AgBF_4$ [6]. All eight phosphines are chemically equivalent, as evident from the single ^{31}P-NMR resonance ($\delta = 21.6$ ppm). The absence of Au-bound phosphine is also evident in the spectrum. The symmetric disposition of the two $\{Pt_2S_2\}$ butterflies with similar Au–S bonds [av. 2.335(2) Å] and the linear

* Corresponding author. Tel./fax: +65-779-1691.
E-mail address: chmandyh@nus.edu.sg (T.S. Andy Hor).
[1] Present address: Research Institute of Photocatalysis, Fuzhou University, Fuzhou, P.R. China.

0022-328X/03/$ - see front matter © 2003 Elsevier B.V. All rights reserved.
doi:10.1016/S0022-328X(03)00697-1

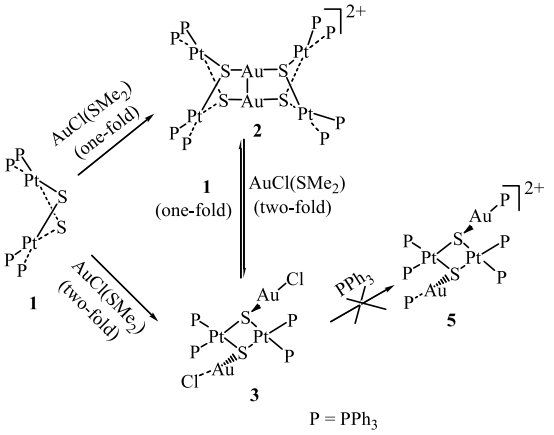

Scheme 1. Preparations and interconversions of $[Au_2\{Pt_2(PPh_3)_4(\mu_3\text{-}S)_2\}_2]Cl_2$, (**2**) and $Au_2Pt_2Cl_2(PPh_3)_4(\mu_3\text{-}S)_2$, (**3**).

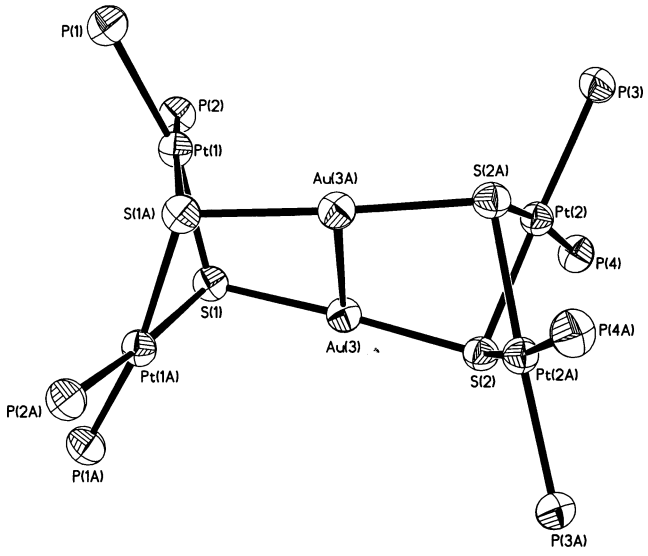

Fig. 1. Thermal ellipsoid plot (50% probability) for $[Au_2\{Pt_2(PPh_3)_4(\mu_3\text{-}S)_2\}_2]^{2+}$, (**2**) (phenyl rings omitted for clarity).

sulfur coordination at Au(I) [S(2)–Au(3)–S(1), 176.08(7)°] facilitate the two Au centers to adopt a T-shape geometry with significant Au–Au bonding. This type of d^{10}–d^{10} M–M interactions at the T-junction has been described in the literature [7]. The Au–Au bond in **2** [2.837 Å] is significantly shorter than that in metallic gold [2.884 Å] [8] and other systems that exhibit aurophilic interactions, e.g. $[Pt_2(PPh_3)_4(\mu_3\text{-}S)_2Au_2(\mu\text{-}dppm)][PF_6]_2$ [2.916 Å] [5]. It should be pointed out that the Au–Au interaction is not a structural imposition for an M_2 anchor on **1a**. This is best exemplified by a similar aggregate $[Pt_2(PPh_3)_4(\mu_3\text{-}S)_2Au_2(\mu\text{-}dppf)][PF_6]_2$ in which the Au···Au separation is nonbonding [3.759 Å] [5]. The flexible and variable M···M distances despite a fairly constant S···S separation (e.g. 3.124 Å in **2**, 3.178 Å in $[Pt_2(PPh_3)_4(\mu_3\text{-}S)_2Au_2(\mu\text{-}dppm)][PF_6]_2$ and 3.128 Å in $[Pt_2(PPh_3)_4(\mu_3\text{-}S)_2Au_2(\mu\text{-}dppf)][PF_6]_2$) and Pt–S–S–Pt dihedral angle [139, 141.4 and 140.5°, respectively] is a functional feature of this system. It helps to ensure that a stable $\{Pt_2S_2\}$ entity is maintained when it receives incoming metal entities of different structural and geometric demands. This is a key value of **1a** in serving as a metalloligand towards a range of metallic and non-metallic substrates. It also demonstrates the structural flexibility of **1a** and explains how it is adaptable to support a range of aggregates and cluster expansion reactions. In **2**, the strong Au–Au interaction has little bearing on other M···M contacts, which remain non-bonding [av. Pt···Pt, 3.353 Å; Pt···Au, 3.673 Å].

Formation of **2** is made possible when a naked Au is available. If the Au(I) substrate has a non-labile ligand such as PPh_3, a monosubstituted complex such as $[Pt_2(PPh_3)_4(\mu\text{-}S)(\mu_3\text{-}S)Au(PPh_3)][PF_6]$ would usually result [5]. Indeed, when two-fold $AuCl(SMe_2)$ is present, both Au atoms tend to settle on different sulfur centers within a $\{Pt_2S_2\}$ core. The linear coordination of Au(I) is maintained by retaining the less labile chloride (compared to Me_2S), thus giving **3**, which was first reported by Bos et al. from **1a** with Au gas [9]. The chloride on **3** however is susceptible to displacement by strong donors such as **1a** to give **2** (Scheme 1). Complexes **2** and **3** are therefore reasonable intermediates to each other, for a synthesis from **1a**, depending on experimental conditions. Attempts to replace chloride by PPh_3 in **3** in an attempt to reach $[Ag_2Pt_2(PPh_3)_6(\mu_3\text{-}S)_2]^{2+}$ (**5**) have hitherto failed. This suggests that the nucleophilicity of the sulfur in **1a** and the thermodynamic stability of **2** both contributed to the conversion of **3** to **2**. Complex **3** is largely insoluble in MeOH, THF, but easily dissolves in CH_2Cl_2. Its $^{31}P\{^1H\}$-NMR spectrum suggests that all the phosphines are equivalent ($\delta = 15.2$ ppm). Its structure, which was reported by Bos et al. [9] resembles the $Ag_2Pd_2Cl_2(dppf)_2(\mu_3\text{-}S)_2$ [10] in which two AgCl tails are leading from either side of a flat Pd_2S_2 core from the sulfur centers. The butterfly is flattened in order to accept two metallic fragments. To verify that this is a general behavior, we have succeeded in synthesizing $Ag_2Pt_2Cl_2(dppf)_2(\mu_3\text{-}S)_2$ (**4**) from $Pt_2(\mu\text{-}S)_2(dppf)_2$ (**1b**) and $AgCl(PPh_3)$ (1:2). Displacement of the phosphine (PPh_3) is preferred to the chloride, thus resulting in a neutral heterometallic aggregate. Accordingly, **4** can also be prepared from **1b** and AgCl (1:2). $^{31}P\{^1H\}$-NMR analysis suggested that all phosphines are Pt-bound and equivalent ($\delta = 23.9$ ppm). X-ray single crystal diffraction analysis of this Ag_2Pt_2 aggregate suggested that it shares a flat $\{Pt_2S_2\}$ plane with the Ag_2Pd_2 and Au_2Pt_2 structures (Fig. 2 and Table 1). It has an ca. C_{2h} symmetry with the Pt–Pt vector as the local twofold axis. The two Pt atoms are merely 0.028 Å above and below the least-square plane defined by the four P atoms. Above and below this plane are two Ag–Cl pendants protruding almost perpendicularly out of the plane, with linear Ag(I) [S(1)–Ag(1)–Cl(1) 178.34°].

Table 1
Selected bond lengths (Å) and angles (°) for $[Au_2\{Pt_2(PPh_3)_4(\mu_3\text{-}S)_2\}_2]Cl_2\cdot\frac{1}{2}H_2O$ (**2**) and $Ag_2Pt_2Cl_2(dppf)_2(\mu_3\text{-}S)_2\cdot 4CH_2Cl_2$ (**4**)

$[Au_2\{Pt_2(PPh_3)_4(\mu_3\text{-}S)_2\}_2]Cl_2\cdot\frac{1}{2}H_2O$ (**2**)			
Pt(1)–P(2)	2.329(2)	Pt(1)–P(1)	2.344(2)
Pt(1)–S(1)	2.368(2)	Pt(1)–S(1A)	2.375(2)
Pt(2)–P(4)	2.319(2)	Pt(2)–P(3)	2.334(2)
Pt(2)–S(2)	2.355(2)	Pt(2)–S(2A)	2.395(2)
Au(3)–S(2)	2.334(2)	Au(3)–S(1)	2.335(2)
Au(3)–Au(3A)	2.837(1)	S(1)–Pt(1A)	2.375(2)
S(2)–Pt(2A)	2.395(2)	S(1)···S(1A)	3.072
S(2)···S(2A)	3.124		
Pt–S–S–Pt	139		
P(2)–Pt(1)–P(1)	99.89(8)	P(2)–Pt(1)–S(1)	89.53(7)
P(1)–Pt(1)–S(1)	164.07(7)	P(2)–Pt(1)–S(1A)	170.24(8)
P(1)–Pt(1)–S(1A)	89.74(7)	S(1)–Pt(1)–S(1A)	80.73(7)
P(4)–Pt(2)–P(3)	98.97(8)	P(4)–Pt(2)–S(2)	90.07(8)
P(3)–Pt(2)–S(2)	169.40(7)	P(4)–Pt(2)–S(2A)	171.47(8)
P(3)–Pt(2)–S(2A)	88.34(7)	S(2)–Pt(2)–S(2A)	82.25(8)
S(2)–Au(3)–S(1)	176.08(7)	S(2)–Au(3)–Au(3A)	92.23(5)
S(1)–Au(3)–Au(3A)	91.67(5)	Au(3)–S(1)–Pt(1)	109.11(8)
Au(3)–S(1)–Pt(1A)	96.22(7)	Pt(1)–S(1)–Pt(1A)	91.08(7)
Au(3)–S(2)–Pt(2)	96.59(7)	Au(3)–S(2)–Pt(2A)	109.16(7)
Pt(2)–S(2)–Pt(2A)	88.69(7)		
$Ag_2Pt_2Cl_2(dppf)_2(\mu_3\text{-}S)_2\cdot 4CH_2Cl_2$ (**4**)			
Pt(1)–P(1)	2.288(2)	Pt(1)–P(2)	2.298(2)
Pt(1)–S(1)	2.354(2)	Pt(1)–S(1A)	2.376(2)
Pt(1)···Ag(1A)	3.061(1)	Pt(1)···Ag(1)	3.111(1)
Ag(1)–Cl(1)	2.335(2)	Ag(1)–S(1)	2.398(2)
Ag(1)···Pt(1A)	3.061(1)	S(1)–Pt(1A)	2.376(2)
Pt(1)···Pt(1A)	3.551(2)	S(1)···S(1A)	3.126(2)
P(1)–Pt(1)–P(2)	97.97(5)	P(1)–Pt(1)–S(1)	91.69(5)
P(2)–Pt(1)–S(1)	169.75(4)	P(1)–Pt(1)–S(1A)	174.34(5)
P(2)–Pt(1)–S(1A)	87.67(5)	S(1)–Pt(1)–S(1A)	82.71(4)
Cl(1)–Ag(1)–S(1)	178.34(7)	Pt(1)–S(1)–Pt(1A)	97.29(4)
Pt(1)–S(1)–Ag(1)	81.77(5)	Pt(1A)–S(1)–Ag(1)	79.75(4)

This additional crystallographic evidence suggested that the flatten-butterfly $\{Pt_2S_2\}$ conformation is sustainable by any combination between {Ag, Au} and {Pd, Pt} or by replacing PPh_3 with a bidentate phosphine like dppf. This generality is useful in our move towards multi-metallic assembly from single metallic source. Unlike **2**, the two metals (Ag) anchored on the $\{Pt_2S_2\}$ core do not interact because they protrude out from opposite sides of the plane. The Ag···Pt separation [av. 3.086(2) Å] is only slightly longer than some documented Ag–Pt bonds [e.g. 2.772(3) and 3.063(3) Å in $(NBu_4)_2[Ag_2Pt_2(C_6F_5)_4Cl_4]$] [11] but these are non-bonding d^{10}–d^8 contacts. Similarly, the Pt···Pt contacts (3.551 Å) are non-bonding. The two C_5 rings of dppf, which are essentially coplanar (dihedral angle $\theta = 3.0°$), adopt a common *staggered* (*gauche*) conformation.

We are currently studying the possibility to use **1**, **3** and **4** to enter into intermetallic aggregates with high-nuclearity. Preliminary experiments suggested that although it was possible to replace the terminal Cl in a similar Hg(II) derivative, $Hg_2(\mu\text{-}Cl)_2Cl_2Pt_2(Ph_3P)_4(\mu\text{-}S)_2$ (*hinged*) by PPh_3 [12], similar replacement attempts on **3** and **4** (*flat*) were futile. The relationship of chemical reactivity to the geometric and conformational behavior remains to be tested further. We have earlier advocated that in a *hinged* conformation, the Pt coordination spheres and M–S bonds are directly coupled, which is absent when the butterfly is *flat* [13]. In a study of $[Ag_2\{Pt_2(PPh_3)_4(\mu_3\text{-}S)_2\}_2]^{2+}$ we also suggested that the two $\{Pt_2S_2\}$ moieties absorb some electron density from the Ag–Ag bond through folding to recoup some of the lost electron density upon coordination [2]. These suggested that the plane conformation of **1a** depends

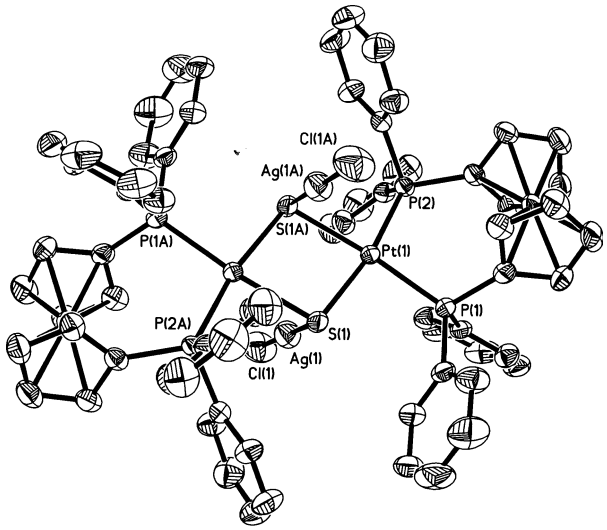

Fig. 2. Thermal ellipsoid plot (50% probability) for $Ag_2Pt_2Cl_2(dppf)_2(\mu_3\text{-}S)_2$ (**4**).

very much on the substituent on the incoming metal as well as the strength of the M···M bond thus formed. There also appears to be little impetus for $\{Pt_2S_2\}$ folding simply for the formation of the weak M–M bond. We need to understand these salient features when we use these complexes as heterometallic molecular precursors to build supramolecular intermetallic materials.

3. Experimental

All reactions were routinely performed under a pure argon atmosphere unless otherwise stated. All solvents were distilled and degassed before use. $Pt_2(PPh_3)_4(\mu\text{-}S)_2$ (**1a**) and $Pt_2(dppf)_2(\mu\text{-}S)_2$ (**1b**) were synthesized from *cis*-$[PtCl_2(P–P)]$ (P–P = 2PPh_3, dppf) and $Na_2S\cdot 9H_2O$ according to a literature method [14]. Elemental analyses were conducted in the Elemental Analysis Laboratory in the Department of Chemistry, National University of Singapore. The $^{31}P\{^1H\}$-NMR spectra were recorded on a Bruker ACF 300 spectrometer with H_3PO_4 as external reference.

3.1. Syntheses

3.1.1. $[Au_2\{Pt_2(PPh_3)_4(\mu_3\text{-}S)_2\}_2]Cl_2$ (**2**)

*3.1.1.1. From **1a** and $AuCl(SMe_2)$.* $AuCl(SMe_2)$ (0.029 g, 0.1 mmol) was added with stirring to a MeOH (40 cm^3) suspension of $[Pt_2(PPh_3)_4(\mu\text{-}S)_2]$, **1a** (0.15 g, 0.1 mmol). The orange suspension changed gradually to an orange solution after stirring for 6 h. Diethyl ether was added to the resultant solution to give an orange precipitate of **2**. The product was recrystallized in CH_2Cl_2–hexane to give yellow crystals. (Yield: 0.085 g, 49%) Anal. Calc. for $C_{144}H_{120}Au_2Cl_2P_8Pt_4S_4$: C, 49.81; H, 3.46; P, 7.15; S, 3.69. Found: C, 48.98; H, 3.68; P, 7.60; S, 3.25%. $^{31}P\{^1H\}$-NMR ($CDCl_3$): δ 21.6 ppm (8P, s, ^1J(P–Pt) 3127 Hz, ^3J(P–Pt) 35 Hz).

*3.1.1.2. From **3** and **1a**.* A suspension of **3** (0.1 g, 0.05 mmol) and **1a** (0.075 g, 0.05 mmol) in 1:1 molar ratio was stirred in THF (40 ml) for 6 h to give a clear yellow solution from which yellow solid of **2** could be isolated (Yield: 0.073 g, 42%).

3.1.2. $Au_2Pt_2Cl_2(PPh_3)_4(\mu_3\text{-}S)_2$ (**3**)

*3.1.2.1. From **1a** and $AuCl(SMe_2)$.* $AuCl(SMe_2)$ (0.058 g, 0.2 mmol) was added with stirring to an orange THF (40 cm^3) suspension of $[Pt_2(PPh_3)_4(\mu\text{-}S)_2]$, **1a** (0.15 g, 0.1 mmol). After 2 h, the resultant yellow suspension was filtered and a yellow precipitate was obtained. The product was recrystallized in CH_2Cl_2–hexane to give yellow crystals (Yield: 0.086 g, 44%).

*3.1.2.2. From **2** and $AuCl(SMe_2)$.* $AuCl(SMe_2)$ (0.029 g, 0.1 mmol) was added with stirring to a THF (40 cm^3) solution of $[Au_2\{Pt_2(PPh_3)_4(\mu_3\text{-}S)_2\}_2]Cl_2$ (0.17 g, 0.05 mmol) and the mixture stirred for 2 h. The resultant yellow suspension was filtered and a yellow precipitate was obtained. The product was recrystallized in CH_2Cl_2–hexane to give yellow crystals. (Yield: 0.102 g, 53%). Anal. Calc. for $C_{72}H_{60}Au_2Cl_2P_4Pt_2S_2$: C, 43.9; H, 3.05; P, 6.31; S, 3.32. Found: C, 43.3; H, 3.12; P, 6.67; S, 3.53%. $^{31}P\{^1H\}$-NMR (CD_2Cl_2): δ 15.2 ppm (4P, s, ^1J(P–Pt) 3006 Hz).

3.1.3. $Ag_2Pt_2Cl_2(dppf)_2(\mu_3\text{-}S)_2$ (**4**)

*3.1.3.1. From **1b** and $AgCl(PPh_3)$.* $AgCl(PPh_3)$ (0.032 g, 0.0776 mmol) was added with stirring to a THF (20 cm^3) suspension of **1b** (0.078 g, 0.0388 mmol). The orange suspension changed gradually to an orange solution after stirring for 2 h. Hexane was added to the resultant solution to give an orange precipitate of complex **4**. The product was recrystallized in CH_2Cl_2–hexane to give orange crystals. (Yield: 0.043g, 59%). Anal. Calc. for $C_{68}H_{56}Ag_2Cl_2Fe_2P_4Pt_2S_2$: C, 44.49; H, 3.05; P, 6.76; S, 3.49. Found: C, 45.10; H, 3.02; P, 5.87; S, 3.24%. $^{31}P\{^1H\}$-NMR ($CDCl_3$): δ 23.9 ppm [4P, s, ^1J(P–Pt) 2980, ^3J(P–Pt) 32 Hz].

*3.1.3.2. From **1b** and AgCl.* AgCl (0.0143 g, 0.1 mmol) was added with stirring to a THF (20 cm^3) suspension of **1b** (0.078 g, 0.05 mmol). The orange suspension changed gradually to an orange solution from which **4** can be isolated. (Yield: 0.048 g, 52%)

3.2. Crystallography

Single crystals of **2** and **4** suitable for X-ray diffraction studies were grown by slow diffusion of hexane to CH_2Cl_2 at room temperature in air. The crystals rapidly turned opaque upon isolation and were hence sealed in a quartz capillary with the mother liquor during data collection. Data collections of crystals of **2** and **4** were carried out on a Siemens CCD SMART system. Details of crystal and data collection parameters are summarized in Table 2.

Table 2
Crystal data and structure refinement for $[Au_2\{Pt_2(PPh_3)_4(\mu_3\text{-}S)_2\}_2]Cl_2\cdot\frac{1}{2}H_2O$ (**2**) and $Ag_2Pt_2Cl_2(dppf)_2(\mu_3\text{-}S)_2\cdot 4CH_2Cl_2$ (**4**)

	2	**4**
Chemical formula	$C_{144}H_{121}Au_2Cl_2O_{0.50}P_8Pt_4S_4$	$C_{72}H_{64}Ag_2Cl_{10}Fe_2P_4Pt_2S_2$
Formula weight	3479.59	2189.35
Crystal system	Monoclinic	Monoclinic
Space group	*C*2/*c*	$P2_1/c$
a (Å)	21.318(2)	12.939(3)
b (Å)	26.112(7)	20.453(2)
c (Å)	25.952(4)	15.679(6)
α (°)	90	90
β (°)	100.33(1)	113.30(1)
γ (°)	90	90
U (Å^3)	14212.7(?)	3811.3(9)
Z	4	2
D_{calc}(g cm^{-3})	1.626	1.908
μ (mm^{-1})	6.212	5.061
F(000)	6704	2120
Theta range for data collection (°)	1.56–27.08	1.71–26.48
h, *k*, *l* range	−20–27, −33–33, −33–33	−16–3, −19–19, −18–19
No.of reflections collected	41704	9789
No. of unique data	14875	6312
Min, max transmission	0.550, 0.862	0.465, 0.862
No. of variables	750	424
Residuals: R_1 [a], wR_2 [b] (obsdata)	0.0415, 0.1108	0.0356, 0.0859
Residuals: R_1 [a], wR_2 [b] (alldata)	0.0642, 0.1232	0.0420, 0.0893
Goodness-of-fit	1.098	1.033
$(\Delta\rho)$max, $(\Delta\rho)$max (e Å^{-3})	1.842, −0.845	1.189, −2.148

[a] $R_1 = \Sigma||F_o|-|F_c||/\Sigma|F_o|$.
[b] $\omega R_2 = \{\Sigma\ \omega[(F_o^2 - F_c^2)^2]/\Sigma\ \omega F_o^4\}^{1/2}$; $\rho = [(F_o^2,\ \theta) + 2F_c^2]/3$.

The structures of **2** and **4** were solved by direct methods and non-hydrogen atoms were located from Fourier difference maps. Full-matrix least-squares refinements were carried out with anisotropic temperature factor for all non-hydrogen atoms. Hydrogen atoms were placed on calculated positions (C–H 0.96 Å) and assigned isotropic thermal parameters riding on their parent atoms. Initial calculations were carried out on a PC using SHELXTL PC software package; SHELXTL-93 was used for the final refinements [15]. Corrections for absorption were carried out by the SADABS method.

4. Supplementary materials

Crystallographic data for the structural analysis have been deposited with the Cambridge Crystallographic Data Centre, CCDC nos. 211621 and 211620 for compounds $[Au_2\{Pt_2(PPh_3)_4(\mu_3\text{-}S)_2\}_2]Cl_2\cdot\frac{1}{2}H_2O$ (**2**) and $Ag_2Pt_2Cl_2(dppf)_2(\mu_3\text{-}S)_2\cdot 4CH_2Cl_2$ (**4**), respectively. Copies of this information may be obtained free of charge from The Director, CCDC, 12 Union Road, Cambridge CB2 1EZ, UK (Fax: +44-1223-336033; e-mail: deposit@ccdc.cam.ac.uk or www: http://www.ccdc.cam.ac.uk/conts/retrieving.html.

Acknowledgements

The authors acknowledge the National University of Singapore (NUS) for financial support. Z. Li thanks NUS for a research scholarship award. Technical support from the Department of Chemistry of NUS is appreciated.

References

[1] S.W.A. Fong, T.S.A. Hor, J. Chem. Soc. Dalton Trans. (1999) 639.
[2] H. Liu, A.L. Tan, C.R. Cheng, K.F. Mok, T.S.A. Hor, Inorg. Chem. 36 (1997) 2916.
[3] X. Xu, S.-W. Fong, Z. Li, Z.-H. Loh, F. Zhao, J.J. Vittal, W. Henderson, S.B. Khoo, T.S.A. Hor, Inorg. Chem. 41 (2002) 6838.
[4] (a) S.H. Chong, T.S.A. Hor, J. Mol. Catal. A: Chem. (2003), in press.;
(b) J.S.L. Yeo, J.J. Vittal, T.S.A. Hor, Euro. J. Inorg. Chem. (2003) 277.
[5] Z. Li, Z. Loh, K.F. Mok, T.S.A. Hor, Inorg. Chem. 39 (2000) 5299.
[6] C.E. Briant, T.S.A. Hor, N.D. Howells, D.M.P. Mingos, J. Organomet. Chem. 256 (1983) C15.
[7] (a) S.L. Lawton, W.J. Rohrbaugh, G.T. Kokotailo, Inorg. Chem. 11 (1972) 2227;
(b) J.K.M. Rao, M.A. Viswamitra, Acta Crystallogr. 28B (1972) 1484;

(c) M.R. Udupa, B. Krebs, Inorg. Chim. Acta 7 (1973) 271;
(d) P. Coggon, A.T. McPhail, J. Chem. Soc. Chem. Commun. (1972) 91.
[8] D.N. Batchelder, R.O. Simmons, Appl. Phys. 36 (1965) 2864.
[9] W. Bos, J.J. Bour, P.P.J. Schlebos, P. Hageman, W.P. Bosman, J.M.M. Smits, J.A.C. van Wietmarschen, P.T. Beurskens, Inorg. Chim. Acta 119 (1986) 141.
[10] G.M. Li, S.H. Li, A.L.C. Tan, W.H. Yip, T.C.W. Mak, T.S.A. Hor, J. Chem. Soc. Dalton Trans. (1996) 4315.
[11] A. Müller, H. Bögge, E. Königer-Ahlborn, Z. Naturforsch B34 (1979) 1698.
[12] Z. Li, X. Xu, S.B. Khoo, K.F. Mok, T.S.A. Hor, J. Chem. Soc. Dalton Trans. (2000) 2901.
[13] A.L. Tan, M.L. Chiew, T.S.A. Hor, J. Mol. Struct. (Theochem) 393 (1996) 189.
[14] R. Ugo, G. La Monica, S. Cenimi, A. Segre, F. Conti, J. Chem. Soc. A (1971) 522.
[15] G.M. Sheldrick, SHELXL-93, Program for Crystal Structure Refinement; University of Göttingen, Germany.